


Framework humanization optimizes potency of anti-CD72 nanobody CAR-T cells for B-cell malignancies

William C Temple ^{1,2,3}, Matthew A Nix,³ Akul Naik,³ Adila Izgutdina,³ Benjamin J Huang,^{1,4} Gianina Wicaksono,³ Paul Phojanakong,⁴ Juan Antonio Camara Serrano,⁴ Elizabeth P Young,¹ Emilio Ramos,³ Fernando Salangsang,⁴ Veronica Steri,⁴ Simayijiang Xirenayi,¹ Michelle Hermiston,^{1,2} Aaron C Logan,⁵ Elliot Stieglitz,¹ Arun P Wiita^{3,6,7}

To cite: Temple WC, Nix MA, Naik A, *et al.* Framework humanization optimizes potency of anti-CD72 nanobody CAR-T cells for B-cell malignancies. *Journal for ImmunoTherapy of Cancer* 2023;**11**:e006985. doi:10.1136/jitc-2023-006985

► Additional supplemental material is published online only. To view, please visit the journal online (<http://dx.doi.org/10.1136/jitc-2023-006985>).

Accepted 17 October 2023

ABSTRACT

Background Approximately 50% of patients who receive anti-CD19 CAR-T cells relapse, and new immunotherapeutic targets are urgently needed. We recently described CD72 as a promising target in B-cell malignancies and developed nanobody-based CAR-T cells (nanoCARs) against it. This cellular therapy design is understudied compared with scFv-based CAR-T cells, but has recently become of significant interest given the first regulatory approval of a nanoCAR in multiple myeloma.

Methods We humanized our previous nanobody framework regions, derived from llama, to generate a series of humanized anti-CD72 nanobodies. These nanobody binders were inserted into second-generation CD72 CAR-T cells and were evaluated against preclinical models of B cell acute lymphoblastic leukemia and B cell non-Hodgkin's lymphoma in vitro and in vivo. Humanized CD72 nanoCARs were compared with parental ("NbD4") CD72 nanoCARs and the clinically approved CD19-directed CAR-T construct tisagenlecleucel. RNA-sequencing, flow cytometry, and cytokine secretion profiling were used to determine differences between the different CAR constructs. We then used affinity maturation on the parental NbD4 construct to generate high affinity binders against CD72 to test if higher affinity to CD72 improved antitumor potency.

Results Toward clinical translation, here we humanize our previous nanobody framework regions, derived from llama, and surprisingly discover a clone ("H24") with enhanced potency against B-cell tumors, including patient-derived samples after CD19 CAR-T relapse. Potentially underpinning improved potency, H24 has moderately higher binding affinity to CD72 compared with a fully llama framework. However, further affinity maturation ($K_D < 1$ nM) did not lead to improvement in cytotoxicity. After treatment with H24 nanoCARs, in vivo relapse was accompanied by CD72 antigen downregulation which was partially reversible. The H24 nanobody clone was found to have no off-target binding and is therefore designated as a true clinical candidate.

Conclusion This work supports translation of H24 CD72 nanoCARs for refractory B-cell malignancies, reveals potential mechanisms of resistance, and unexpectedly demonstrates that nanoCAR potency can be improved by framework alterations alone. These findings may have

WHAT IS ALREADY KNOWN ON THIS TOPIC

⇒ Our group recently demonstrated that CD72 is a promising, previously unexplored immunotherapy target for B cell malignancies, and that nanobody-based anti-CD72 chimeric antigen receptor T cells (CD72 nanoCARs) have potent antitumor efficacy in preclinical models.

WHAT THIS STUDY ADDS

⇒ Of many factors known to impact CAR-T cell efficacy, the role of the antigen recognition domain is relatively understudied. Here, we find that framework humanization of anti-CD72 nanobodies lead to enhanced antitumor potency of CD72 nanoCARs, potentially due to enhanced binding affinity to CD72, compared with the original anti-CD72 nanobody sequence. This work describes preclinical characterization and development of a novel cellular therapy, while also informing CAR design principles.

HOW THIS STUDY MIGHT AFFECT RESEARCH, PRACTICE OR POLICY

⇒ This study motivates a future, first-in-human phase 1 clinical trial evaluating humanized CD72 nanoCARs in patients with CD72+ B cell malignancies who do not respond to CD19 CAR-T cell therapy.

implications for future engineering of nanobody-based cellular therapies.

INTRODUCTION

Engineered cellular immunotherapies such as CD19 chimeric antigen receptor T cells (CAR-T cells) have emerged as a central pillar of oncologic care for patients with relapsed and refractory B cell malignancies. Though complete remission is achieved in 70%–90% of B-cell acute lymphoblastic leukemia (B-ALL) or non-Hodgkin's lymphoma (NHL) patients who receive CD19 CAR-T cells, only ~50% remain in remission 1 year after treatment.^{1–3} Outcomes for patients who relapse



© Author(s) (or their employer(s)) 2023. Re-use permitted under CC BY-NC. No commercial re-use. See rights and permissions. Published by BMJ.

For numbered affiliations see end of article.

Correspondence to

Dr Arun P Wiita;
arun.wiita@ucsf.edu

after CD19 CAR-T cell therapy are dismal and remain an unmet medical need.^{4–6} CD22 CAR-T cells are under investigation as a second-line cellular therapy strategy, but these therapies appear only rarely curative and are typically used clinically as a bridge to allogeneic stem cell transplant.⁷ New immunotherapeutic targets are urgently needed to provide additional alternatives after CD19 CAR-T relapse.

Our laboratory recently identified CD72 as a promising immunotherapy target upregulated in *KMT2A*-rearranged B-ALL, with subsequent work suggesting that CD72 was expressed on essentially all genomic subtypes of B-ALL as well as B-cell NHL patient samples.⁸ CD72 is a B-cell-restricted, highly expressed surface antigen that is an inhibitor of the B cell receptor signaling complex.⁹ In this previous work, we developed a fully synthetic nanobody against CD72 (“NbD4”) using a yeast display platform, demonstrating that NbD4 nanobody-based CAR-T cells (nanoCARs) are efficacious in vitro and in vivo.⁸ Loss of CD19 on B-ALL models did not alter CD72 expression and NbD4 nanoCARs remained effective at eliminating these tumors.⁸ In vivo, however, we found that NbD4 nanoCARs were consistently less potent than single chain variable (scFv)-based CD19 CAR-T when both were equipped with an equivalent 4-1BB costimulatory domain in the CAR backbone. Therefore, we sought to employ iterative CAR engineering to improve anti-CD72 nanoCARs prior to clinical translation.

While modification of domains related to CAR signaling has been extensively investigated, much less is known about how modifications of the binding domain impact CAR phenotypes. Nanobodies (V_{HH}), derived from llama heavy chain-only antibodies, are obligate monomers. However, the great majority of previously investigated CAR-T cells incorporate an scFv for antigen recognition, comprising a linked heterodimer of a variable heavy and variable light (V_H and V_L) chain.^{10–11} Toward discerning relevant properties of antibody fragment design in CARs, some groups have hypothesized that the affinity of an scFv may impact CAR-T potency.^{12–13} Specifically, Ghorashian *et al* tested low affinity (~ 15 nM K_D) CD19 “CAT” CAR-T cells and found that they had enhanced persistence in vivo and increased in vitro cytotoxicity compared with traditional high-affinity (< 1 nM K_D) FMC63-based CD19 CAR-T.¹⁴ Notably, the FMC63 scFv clone is used in all current FDA-approved CD19 CAR-T cell products. These findings suggest that tuning the binding affinity of the antigen recognition domain can have a profound impact on downstream CAR function and persistence.

It is unknown if similar features apply to nanobody-based CAR-T cells. Investigation of this question has become highly relevant, as ciltacabtagene autoleucel (“cilta-cel”), a CAR-T cell targeting BCMA for relapsed/refractory multiple myeloma,¹⁵ was recently FDA approved. This cell therapy product, based on a biepitopic nanobody design¹⁶ demonstrated a favorable safety profile and impressive clinical responses when compared with scFv-based CAR-T cells.¹⁷ Given the success of cilta-cel,

numerous additional nanobody-based CAR-T cells,^{10–16} or CAR-T cells incorporating other related “single domain binders”,^{18–20} are under preclinical investigation for a variety of indications. Notably, studies of recombinant proteins have suggested that nanobodies may have higher stability than scFv’s while achieving similar target affinity and specificity.¹⁰ High specificity is critical for use in CAR-T to avoid off-target cytotoxicity to essential tissues. As obligate monomers, nanobodies may lead to reduced CAR-CAR interactions at the T-cell surface, decreasing tonic signaling and T-cell exhaustion versus V_H - V_L interactions across neighboring scFv’s.¹⁰ Finally, scFv’s require a synthetic linker between V_H and V_L domains, leading to an additional potential source of immunogenicity.²¹ For all of these reasons, nanobody-based CAR-Ts may provide advantages over scFv-based CAR-Ts.

Among several proposed mechanisms by which CD19 CAR-T fails in patients, one is the development of anti-drug antibodies versus the murine-derived scFv.^{21–23} Here, we thus sought to reduce potential immunogenicity of the NbD4 nanobody via framework humanization. The goal of this strategy, commonly used in protein engineering, is to reduce immunogenicity of the therapeutic product in humans.¹⁰ This method is used to mutate specific amino acids in the framework (constant) regions of the llama-derived nanobody sequence to be identical to the equivalent human residues, while keeping the complementarity-determining regions (CDRs, unique sequences that lead to specificity of antigen recognition) unchanged.

Surprisingly, during this humanization process, we unexpectedly found that one sequence clone (“H24”) significantly increased CAR potency against B cell malignancy lines in vitro and in vivo. We found that H24 showed moderately increased binding affinity versus NbD4, potentially underlying this increased potency; however, further maturation to much higher-affinity binders did not markedly improve CAR-T cell activity, in line with prior findings with scFv-based CAR-T cells.^{14–24–25} In preclinical evaluation, the H24 nanobody showed high specificity for CD72 and favorable antitumor effects compared with CD19 CAR-T. To our knowledge, it has not previously been demonstrated that framework mutations of a nanobody CAR binder alone can enhance CAR potency in vitro and in vivo. Collectively, our evaluation suggests that H24 CD72 nanoCARs are both potent and safe, supporting clinical translation of this potentially promising new cellular therapy for patients at the highest risk of morbidity and mortality from aggressive B cell malignancies.

MATERIALS AND METHODS

CAR engineering

Empty CAR, CD19, and NbD4 CAR expression plasmids used identical components aside from the variable extracellular binding domains (no binder for empty CAR, CD19-directed scFv with clone FMC63, or CD72 directed

parental nanobody NbD4). The CD8 hinge and transmembrane domain, 4-1BB costimulatory domain, and CD3 ζ signaling domain are identical to those used in the clinically approved CD19-directed CAR construct tisagenlecleucel. H24 nanoCAR expression plasmid included the H24 anti-CD72 nanobody binder, an IgG4 hinge region mutated to avoid Fc receptor interaction (“EQ”)²⁶ a CD28 transmembrane domain, and a CD28 costimulatory domain. All humanized binders and affinity matured nanoCARs used identical CAR backbones to the H24 nanoCAR construct. Additional details are in online supplemental methods.

Lentiviral vector production

Lenti-X 293T cells were transfected with each CAR expression plasmid, cultured for 2–3 days, and then lentivirus harvested. Primary human T cells were transduced with lentivirus. Additional details in online supplemental methods.

CAR-T in vitro cytotoxicity assays

Cytotoxicity assays were conducted by mixing target cells with CAR-T cells for 24 hours using the indicated effector:tumor (E:T) ratios. For measuring cytotoxicity by bioluminescence with target cell lines stably expressing effLuc, 150 μ g/mL of d-luciferin (Gold Biotechnology, LUCK-1G) was added to each sample, incubated for 10 min at room temperature, and then read using a GloMax Explorer Plate Reader (Promega). Additional details are available in online supplemental methods.

Murine experiments

NSG (NOD.Cg-Prkdc^{scid} Il2rg^{tm1Wjl}/SzJ, Jackson Laboratories) strain mice were used for all experiments. Mice were infused via tail-vein injection with 1e6 SEM B-ALL cells or 5e5 JeKo-1 NHL cells. Tumor burden was quantified via non-invasive bioluminescence imaging. Mice received either CAR-T cells via tail-vein injection. Symptomatic disease was the survival endpoint. Additional details are in online supplemental methods.

Biolayer interferometry

Biolayer interferometry data (BLI) were obtained using an Octet RED384 (ForteBio) instrument. Biotinylated CD72 protein was loaded onto a streptavidin biosensor, and after blocking with 10 μ M biotin, each of nanobody was added to determine binding affinity. Additional details are in online supplemental methods.

Statistical analysis

All statistical analyses were performed in GraphPad Prism V.9. Data are presented as mean \pm SD, unless otherwise specified. Statistically significant differences are included in each figure and/or figure legend. All n values given are biological replicates, unless otherwise specified. A $p < 0.05$ was considered statistically significant.

RESULTS

Optimizing the CD72 nanoCAR backbone construct

Our original description of the CD72 nanoCAR incorporated the anti-CD72 nanobody clone “NbD4” with a

4-1BB-based backbone with CD8 hinge and transmembrane domain, designed to be analogous to that in the FDA-approved, commercially available anti-CD19 product tisagenlecleucel. As a first step toward product optimization, we sought to investigate whether alternate backbone designs may improve in vivo CD72 nanoCAR potency. Recent work demonstrated that a mutated IgG4 (EQ) hinge sequence with CD28 costimulatory domain was most efficacious in a glioblastoma CAR-T model.²⁷ We investigated this backbone with an NbD4 binder (NbD4.EQ.28z) in comparison to the prior tisagenlecleucel backbone (NbD4.bbzb) and a construct with CD28 hinge+transmembrane+costimulatory domain (NbD4.CD28z), similar to that in axicabtagene ciloleucel and brexucabtagene autoleucel. In in vitro cytotoxicity assays, NbD4.EQ.28z eliminated JeKo-1 lymphoma and NALM6 B-ALL tumors at lower E:T ratios than NbD4.CD8bbzb and NbD4.28bbzb nanoCARs (online supplemental figure 1A). In an in vivo model of JeKo-1 tumor implanted intravenously in NOD *scid* gamma (NSG) mice (1e6 tumor cells at day -4, 4e6 CAR-T cells at day 0) we found that the EQ.28z backbone again outperformed comparators in both survival and tumor burden (online supplemental figure 1B-D). Indeed, these mice did not develop discernible tumor burden even on rechallenge with 1e6 JeKo cells at day 52 (online supplemental figure 1C). Based on these results, we moved forward with the EQ.28z backbone for further preclinical optimization.

Humanized CD72 nanoCARs have potent anti-tumor efficacy and improve on parental NbD4 nanoCAR efficacy

Toward assessing potential immunogenicity, sequence analysis demonstrated the llama-derived framework of NbD4 showed ~82% homology to the framework of a fully human IgG4 variable heavy chain fragment (online supplemental figure 2A). This degree of homology is markedly higher than that of the murine-derived FMC63 scFv (~63% homology) used in commercially available CD19 CAR-T cell products. Therefore, while risk of immunogenicity appears lower than murine scFv binders at baseline, further framework humanization of the anti-CD72 nanoCAR binder may still provide an opportunity to further minimize this risk.

We thus developed a strategy integrating several mutations described in prior reports of nanobody framework humanization.²⁸ Notably, in these experiments, the CDRs were all identical to the parental NbD4 (figure 1A). We first tested 18 humanized framework sequence variants for in vitro cytotoxicity versus the *KMT2A*-rearranged B-ALL model SEM. Patients with *KMT2A*-rearranged B-ALL have dismal outcomes, and our prior work described that CD72 is specifically upregulated in these tumors. We, therefore, used the SEM line as an initial filter to determine the anti-tumor efficacy of CD72 nanoCARs.⁸ We found a wide range of efficacies, with many humanized variants showing decreased CD72 nanoCAR cytotoxicity in 24-hour co-culture assays, but some performing with similar or possibly improved efficacy compared

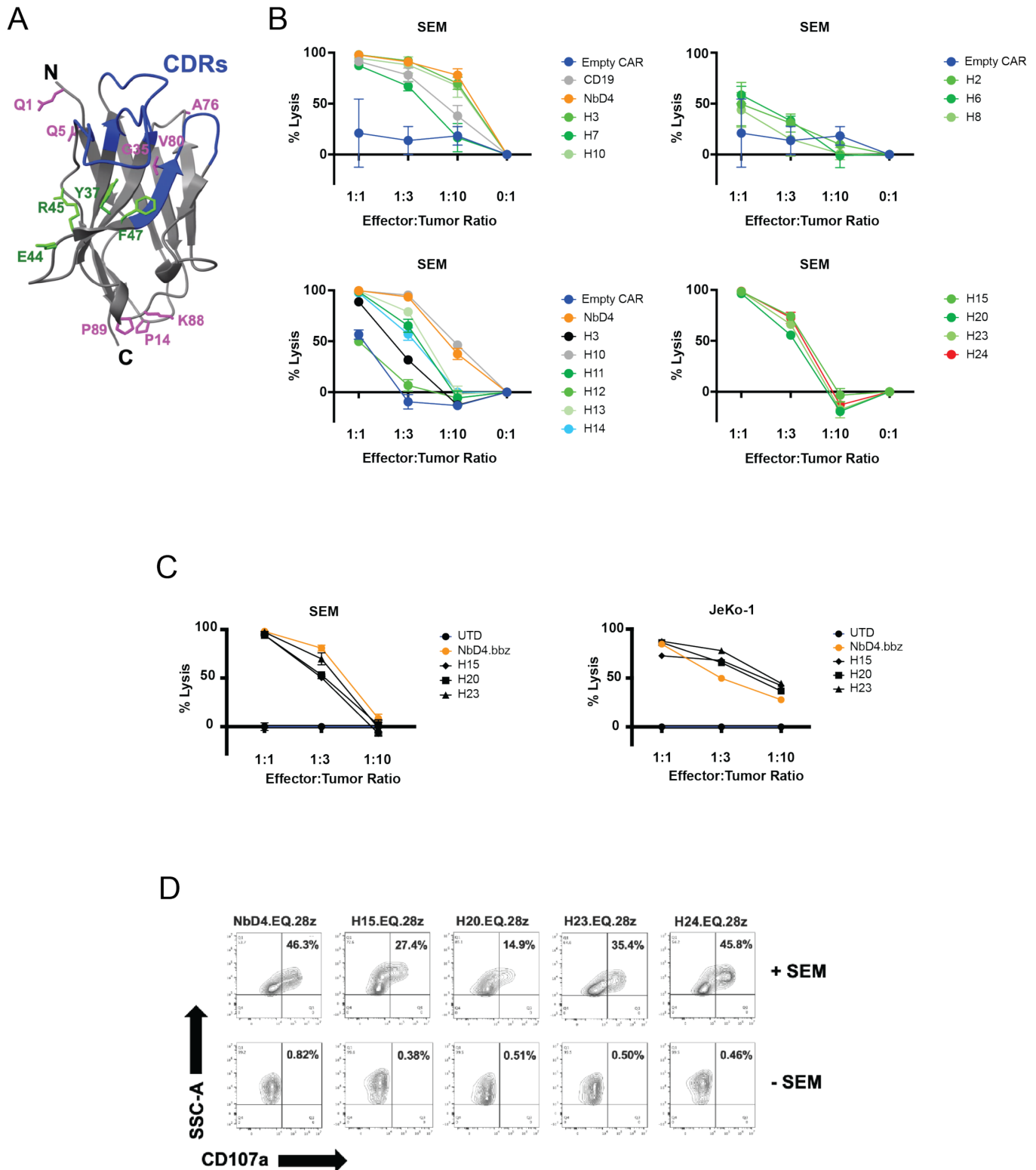


Figure 1 Humanized CD72 nanoCARs have potent anti-leukemia and lymphoma efficacy in vitro. (A) Structural model of the H24 nanobody, in which the framework amino acid substitutions that differentiate NbD4 from H24 are shown in purple. Green amino acids cannot be mutated to human without disrupting obligate monomer nature of nanobody and thus remain as llama-derived sequence in H24. Blue regions represent complementary determining regions (CDRs). Protein structural model created with RaptorX software.⁴⁹ (B) In vitro cytotoxicity assays of various humanized anti-CD72 nanoCARs against *KMT2A*-rearranged B-ALL (SEM). Data are normalized to untransduced T cells (UTD). $n=3$ technical replicates per data point. (C) In vitro cytotoxicity assays of various humanized anti-CD72 nanoCARs against mantle cell lymphoma (JeKo-1). Data are normalized to untransduced T cells. $n=3$ technical replicates. (D) Humanized anti-CD72 nanoCARs were co-cultured in the presence or absence of SEM tumor cells for 24 hours, and then flow cytometry was used to determine degranulation by CD107a expression ($n=1$). B-ALL, B cell acute lymphoblastic leukemia.

with the parental NbD4 sequence (figure 1B; Online supplemental figure 2B). Notably, the binder with the highest homology to human (H6, 95% homology) almost completely abrogated nanoCAR efficacy (figure 1B). We further probed a subset of variants from our initial screen above for cytotoxic efficacy against both JeKo-1 and SEM tumor cells (figure 1C), with “H15”, “H20”, and “H23” all showing favorable performance versus the parental NbD4 sequence. We also profiled CAR-T cell memory/stem-ness markers, based on CD62L/CD45RA staining, finding overall similar characteristics of these humanized sequences to the parental NbD4 both pretumor and post-tumor exposure (online supplemental figure 3A,B). Cytokine release profiling after SEM or JeKo-1 exposure suggested that H23 in particular showed increased TNF α , IL-2, IL-4 and IL-10 secretion compared with parental NbD4 (online supplemental figure 4A,B). For additional variants, we separately evaluated the in vitro phenotype of T-cell degranulation, an important determinant of CAR-T potency, as measured by CD107a expression after 24 hours of co-culture. We found particularly strong degranulation of the H24 sequence variant (89% human framework) compared with NbD4 (82% human) (figure 1D).

Further in vitro cytotoxicity testing revealed H24 to show superior efficacy over NbD4 in repeat antigen stimulation assays (figure 2A) versus both SEM and JeKo-1 cells (figure 2B,C and online supplemental figure 4C). To further investigate the properties of the H24 nanoCAR, we investigated in vitro cytotoxicity using a live-cell imaging (Incucyte) platform. In both SEM and JeKo-1 cell line models, we found that H24 nanoCARs led to either equal or more rapid tumor elimination kinetics than CD19 CAR-T or parental NbD4 nanoCARs (figure 2D,E).

Integrating these analyses, we focused on the “H23” and “H24” sequence variants as candidates for further investigation. These nanobody framework regions have 90% and 89% homology to equivalent human sequence, respectively. Collectively, these data suggest that nanobody framework mutations (alone), without changing the CDRs, can have a marked impact on anti-tumor activity and immunophenotypes of CD72 nanoCARs.

H24 nanoCARs prolong survival of in vivo KMT2A-rearranged B-ALL models and can eliminate B-ALL patient tumors relapsed after CD19 CAR-T cells

As an initial evaluation of in vivo efficacy, to resolve differences between constructs we performed a low-dose CAR “stress test” of H23.EQ.28z and H24.EQ.28z CD72 nanoCARs in comparison to the parental NbD4 sequence (NbD4.bbz), NbD4.EQ.28z, anti-CD19 CAR-T cells (positive control; tisagenlecleucel-analogous backbone, as in our prior study, used as gold-standard clinical comparator,^{2, 29} and “empty” (no binder sequence) control CAR-T (figure 3A). In this study, 1e6 SEM B-ALL cells were implanted on Day -7 with 1.5e6 CAR-T cells administered on day 0. Based on bioluminescence imaging, we found that while CD19 and H24-based CAR-T led to equivalent tumor control at an early time point (Day 12;

figure 3A,B), H24 nanoCARs ultimately led to prolonged tumor control and significantly improved survival versus all other tested CAR-T constructs, including CD19 CAR-T ($p=0.0027$; figure 3C). At this low (“stress”) dose, neither NbD4 nanoCARs nor CD19-based CAR-T prolonged survival versus empty control. This finding suggested that the H24 humanized variant is superior to H23 and could also improve efficacy over the parental NbD4 sequence. This conclusion was supported by a further short-term in vivo study comparing H24.EQ.28z versus various NbD4 constructs, where H24 nanoCARs outperformed all NbD4 constructs at day 6, and showing equivalent B-ALL control to CD19 CAR-T (online supplemental figure 4D,E).

We anticipate that patients most likely to benefit from CD72 nanoCAR therapy are those who relapse after, or do not respond to, CD19 CAR-T. We thus evaluated ex vivo cytotoxicity of H24 nanoCARs against patient B-ALL specimens relapsed after CD19 CAR-T (online supplemental table 2). First, for a pediatric B-ALL tumor we established a patient-derived xenograft model and extracted tumor from murine splenocytes. In this relapsed specimen, we importantly noted that CD19 expression was negative while CD72 expression was preserved (figure 3D). H24 nanoCARs had potent antitumor efficacy against this CD19^{neg}CD72^{pos} B-ALL sample, while CD19 CAR-T had negligible cytotoxicity (figure 3E,F). CD72 had similar expression to CD19 in two adult post-CD19 CAR-T B-ALL specimens, and CD72 notably had higher expression than CD22 in both samples (figure 3G,H). H24 nanoCARs were also superior at eliminating adult primary B-ALL tumors that had relapsed after CD19 CAR-T (figure 3I).

In separate analyses, H24 nanoCARs had similar in vitro proliferation kinetics to CD19 CAR-T against both SEM and JeKo-1 tumors (online supplemental figure 5A,B). H24 nanoCARs and CD19 CAR-T also had similar in vivo persistence in murine peripheral blood against SEM tumors (online supplemental figure 5C).

Taken together, the data above are consistent in establishing the superior potency of humanized H24-based nanoCARs over the parental NbD4-based nanoCARs. In addition, H24 EQ.28z nanoCARs appear to have similar if not somewhat improved efficacy versus CD19.bbz (clinical gold standard) CAR-T, both in vitro and in vivo in the tested models as well as ex vivo versus CD19 CAR-T relapsed B-ALL specimens. These data confirm that nanobody framework humanization can lead to significantly improved characteristics of CD72 nanoCARs. We, therefore, moved forward with the H24 sequence as our lead candidate.

H24 nanoCARs exhibit a unique transcriptional profile compared with CD19 CAR-T cells after exposure to SEM

Given our results above, we hypothesized that H24 nanoCARs and CD19 CAR-T in a tisagenlecleucel backbone may employ different transcriptional programs to eliminate tumors. To study these dynamics, we used bulk RNA-sequencing (RNA-seq) on CAR-T cells before and after SEM co-culture in vitro. We first evaluated expression of

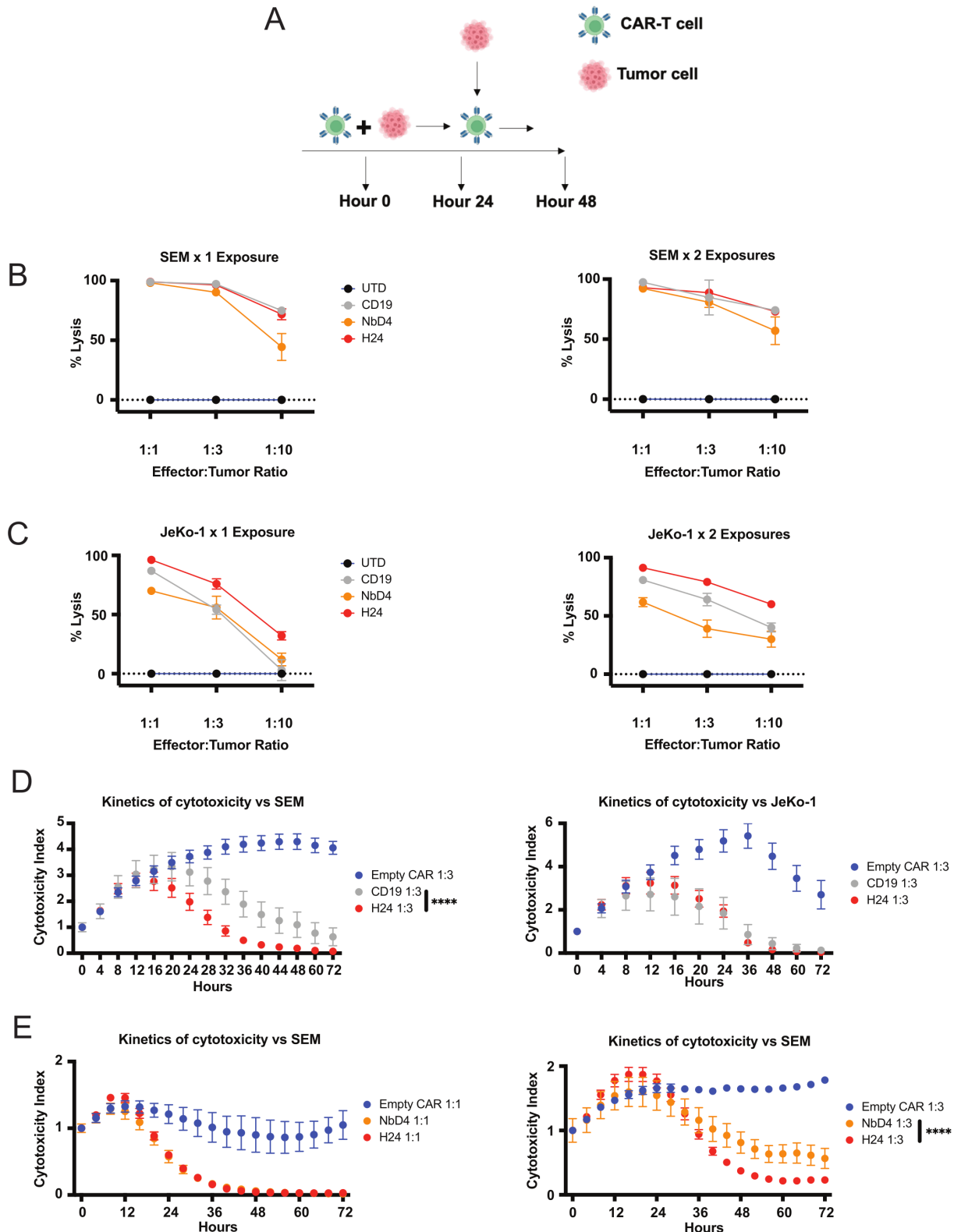


Figure 2 H24 nanoCARs have enhanced antitumor potency versus NbD4 nanoCARs and are non-inferior to CD19 CAR-T cells. (A) Experimental design for the tumor rechallenge experiments. (B) In vitro 24-hour cytotoxicity assays comparing H24, NbD4, and CD19 CAR-T cells against SEM and JeKo-1. Data are normalized to untransduced T cells (UTD). $n=6$ technical replicates. (C) CAR-T cells from [figure 2B](#) were exposed again to SEM tumor at 24 hours at noted E:T ratio. $n=6$ technical replicates. (D) Empty CAR, H24 nanoCARs, and CD19 CAR-T cells were cocultured with SEM or JeKo-1 tumor cells at 1:3 E:T ratio for 72 hours; data obtained using Incucyte live-cell imaging ($n=6$). (E) Empty CAR, H24 nanoCARs, and CD19 CAR-T cells were co-cultured with SEM tumor cells at either a 1:1 or 1:3 E:T ratio for 72 hours using Incucyte. $n=6$ technical replicates. Data in [figure 2D](#) and [figure 2E](#) are generated using two-way ANOVA for multiple comparisons. **** $p<0.0001$. ANOVA, analysis of variance.

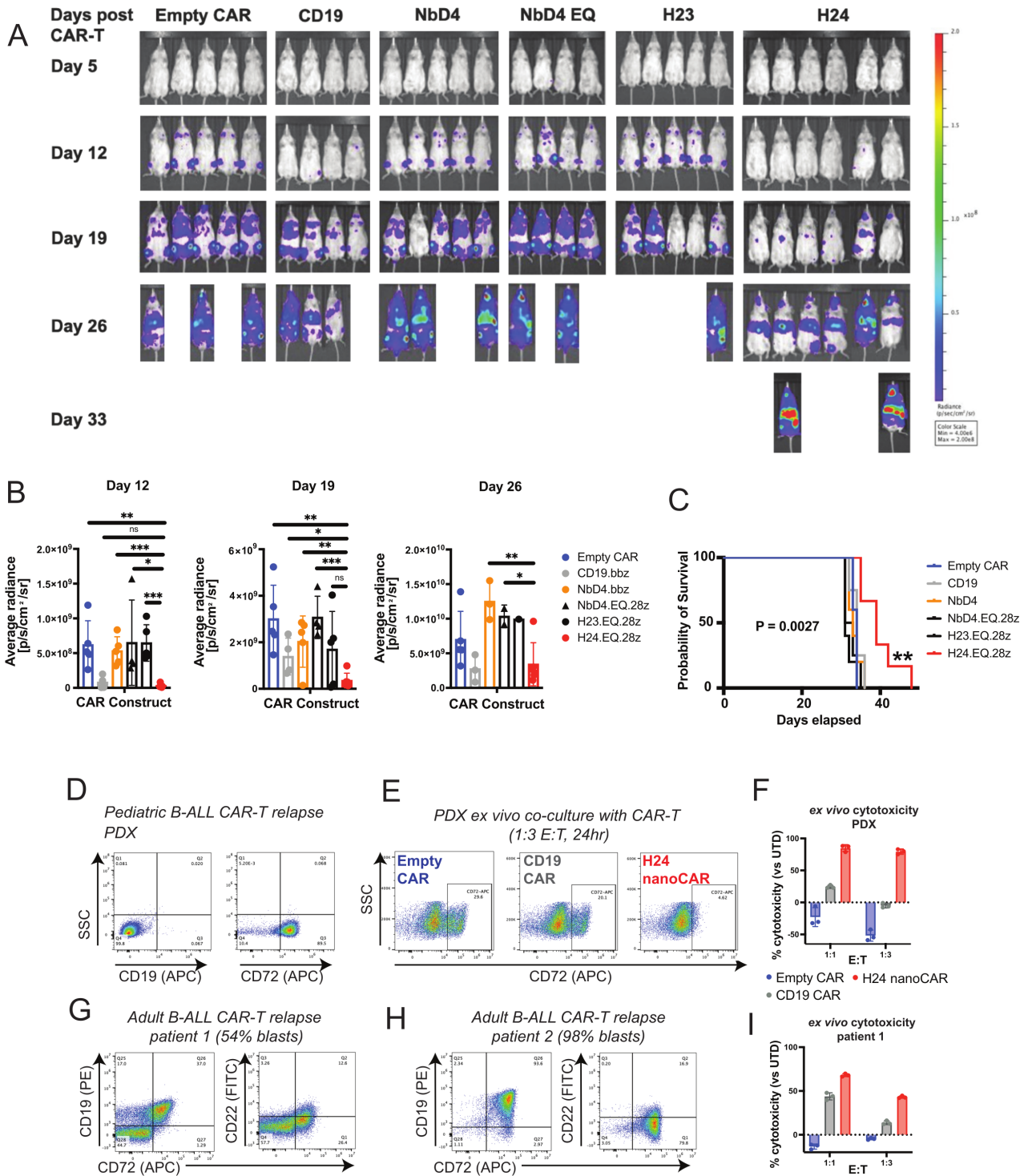


Figure 3 H24 nanoCARs prolong survival in mice implanted with *KMT2Ar* B-ALL tumor and eliminate pediatric and adult B-ALL tumors relapsed after CD19 CAR-T cell therapy. (A) NSG mice were injected with 1×10^6 luciferase-labeled SEM B-ALL cells on day -7, and on day 0 mice were treated with a low-dose in vivo CAR stress test with 1.5×10^6 CAR-T cells per mouse; CAR design as noted per arm. $n=4-6$ mice per arm. (B) Tumor burden assessed weekly via BLI; quantified BLI intensity shown. (C) Kaplan-Meier curves of overall survival. (D) Flow cytometry for CD19 or CD72 was performed on B-ALL PDX splenocytes, derived from a pediatric patient relapsed after CD19 CAR-T cell therapy (representative of $n=3$). (E) H24, CD19, or empty CAR-T cells were cocultured ex vivo with PDX splenocytes for 24 hours. Flow cytometry was performed against CD72 to assess tumor cytotoxicity ($n=3$). (F) Ex vivo cytotoxicity for the various CAR-T cell constructs versus PDX sample, assessed by flow cytometry; percent cytotoxicity normalized to untransduced T cells ($n=3$). (G, H) Flow cytometry for CD19, CD72, and CD22 was performed on two adult B-ALL patient samples relapsed after CD19 CAR-T cell therapy. (I) Ex vivo cytotoxicity versus adult patient sample #1, performed as in (E) ($n=3$). Insufficient sample was available for sample #2 to perform cytotoxicity assay. Data in [figure 3B](#) are generated using an unpaired two-tailed t-test. Data in [figure 3C](#) generated using the log-rank (Mantel-Cox) test. ns= $p < 0.05$, ** $p < 0.01$, *** $p < 0.001$. B-ALL, B cell acute lymphoblastic leukemia; ns not significant.

sentinel T cell transcription factors, as recently compiled by Wu *et al.*,³⁰ pretumor and post-tumor exposure, finding potential increases in transcripts associated with cytotoxicity (*IFNG*, *GZMH*), specific cytokines (*IL-4*, *IL-21*), and inhibitory markers (*CTLA4*, *TIGIT*), for H24 nanoCARs versus CD19 CAR-T post-tumor exposure (figure 4A). We next used Gene Set Enrichment Analysis (GSEA) to evaluate alterations in the broader set of expressed transcripts. We confirmed significantly increased signatures of IFN γ signaling (figure 4B; $p < 0.001$, FDR 0.026) and T-cell receptor signaling (figure 4C; $p < 0.001$, FDR 0.017) in H24 versus CD19 post-tumor. GSEA also confirmed that pathways in cytokine signaling, IL-4, IL-2, and interferon stimulated genes are also upregulated in H24 nanoCARs compared with CD19 after tumor exposure (online supplemental figure 6A). To validate these RNA-seq findings, we cocultured CAR-T cells with SEM or JeKo-1 tumors and found that H24 nanoCARs secrete high levels of cytokines involved in tumor elimination by CAR-T (figure 4D,E; Online supplemental figure 6B). To evaluate pretumor and post-tumor expression of memory/stem-ness phenotypes of H24 nanoCARs, NbD4 nanoCARs, CD19 CAR-T, and empty CAR-T control, we stained for CD45RA and CD62L. After exposure to SEM, the number of naïve T cells was similar between H24, NbD4, and CD19 CAR-T cells. After exposure to JeKo-1 tumors, H24 nanoCARs appeared to show moderately decreased naïve T-cell (Tn) phenotypes and increased T-effector memory RA (TEMRA) cells (figure 4F,G).

We further evaluated alterations in individual genes related to numerous CAR-T phenotypes,³¹ ranging from cytolytic function to exhaustion to persistence (online supplemental figure 6C-I). Given the trend toward increased expression of inhibitory receptors by RNA-seq, PD1, TIM3, and LAG3 were further assessed by flow cytometry. The expression of these exhaustion markers was not significantly different between CD19 CAR-T and H24 nanoCARs (online supplemental figure 7A,B). CD62L expression, a marker of memory qualities, is higher in H24 nanoCARs compared with NbD4 but less than CD19 CAR-T (online supplemental figure 7C). Taken together, these findings suggest that H24 nanoCARs demonstrate increased cytolytic capacity compared with CD19 CAR-T, though potentially with mildly increased inhibitory receptor expression. Our findings are reinforced by studies suggesting the different CD28 and 4-1BB costimulatory domains may lead to differential CAR-T transcriptional programs.^{29,32} Here, these differences appear likely to reflect the changes in the CAR backbone, antibody binder, and target.

H24 nanoCARs lead to persistent CD72 antigen loss in vivo

We next sought to investigate potential mechanisms of resistance to H24 nanoCARs, as understanding such processes will be highly relevant to future clinical translation of this product. For CD19 CAR-T, numerous such mechanisms of resistance have been described, including splicing aberrations leading to loss of the FMC63

epitope,^{33,34} CD19 antigen downregulation,³⁵ anti-murine scFv antibodies,^{21–23} lineage switch,^{36,37} and immune microenvironment-based CAR-T suppression,^{38,39} among others.⁴⁰ We therefore pursued a follow-up in vivo study using the JeKo-1 model implanted intravenously in NSG mice (figure 5A). We found that H24 nanoCARs again outperformed NbD4 nanoCARs in tumor control (figure 5B), though in this specific study CD19 CAR-T cells outperformed both anti-CD72 nanoCARs. Mouse weight across the course of the study was similar between CD19 CAR-T cells and H24 and NbD4 nanoCARs (online supplemental figure 8). After appearance of symptomatic disease, mice were sacrificed and splenocytes harvested for flow cytometry. Immediately after relapse, CD72 antigen expression was significantly downregulated on tumor cells in the nanoCAR-treated arms ($p < 0.001$ vs CD19-treated arm or JeKo-1 cells in culture by t-test) (figure 5C).

To probe the dynamics of this antigen downregulation, we subsequently implanted tumor cells from relapsed nanoCAR-treated mice into a new cohort of tumor-naïve NSG mice. We sacrificed this secondary implant cohort at day 29 post-JeKo-1 infusion (figure 5D). While the sample size is small, precluding firm conclusions, we found that both of the re-implanted mice following NbD4 treatment quickly regained wild type CD72 levels on JeKo-1, while 2 of 3 reimplanted mice following H24 relapse maintained very low CD72 levels (figure 5D). These findings suggest that even in the absence of ongoing immune pressure, CD72 antigen loss induced by H24 nanoCARs may be of a lasting duration, whereas the less potent NbD4 nanoCARs lead to a more rapidly reversible phenotype after the end of treatment. Furthermore, these results emphasize that antigen downregulation may be an important mechanism of resistance to be considered, and potentially overcome, in the context of clinical translation of anti-CD72 nanoCARs.

H24 has moderately increased binding affinity for CD72 compared with NbD4

Given more potent antitumor efficacy and more persistent CD72 suppression in murine models, we hypothesized that the H24 nanobody may have altered biophysical characteristics compared with the parental NbD4. We, therefore, purified each of these recombinant nanobodies as an Fc-domain fusion protein. BLI demonstrated that H24 has a moderately, but significantly, higher binding affinity for recombinant CD72 extracellular domain than NbD4 (K_D 33.0 \pm 0.04 nM vs 50.4 \pm 0.05 nM, respectively) (figure 6A). Notably, these results are consistent with prior studies of CD19-binding scFv's, suggesting that binding affinities in the double-digit nM range may be most efficacious in CAR-T format.¹⁴ To validate the BLI using an orthogonal approach, biotinylated recombinant CD72 protein was added to nanoCAR-expressing T cells at different doses. Gating on the CAR+T cell population, with equivalent CAR expression based on intracellular GFP tag, we found that H24 nanoCARs led to significantly

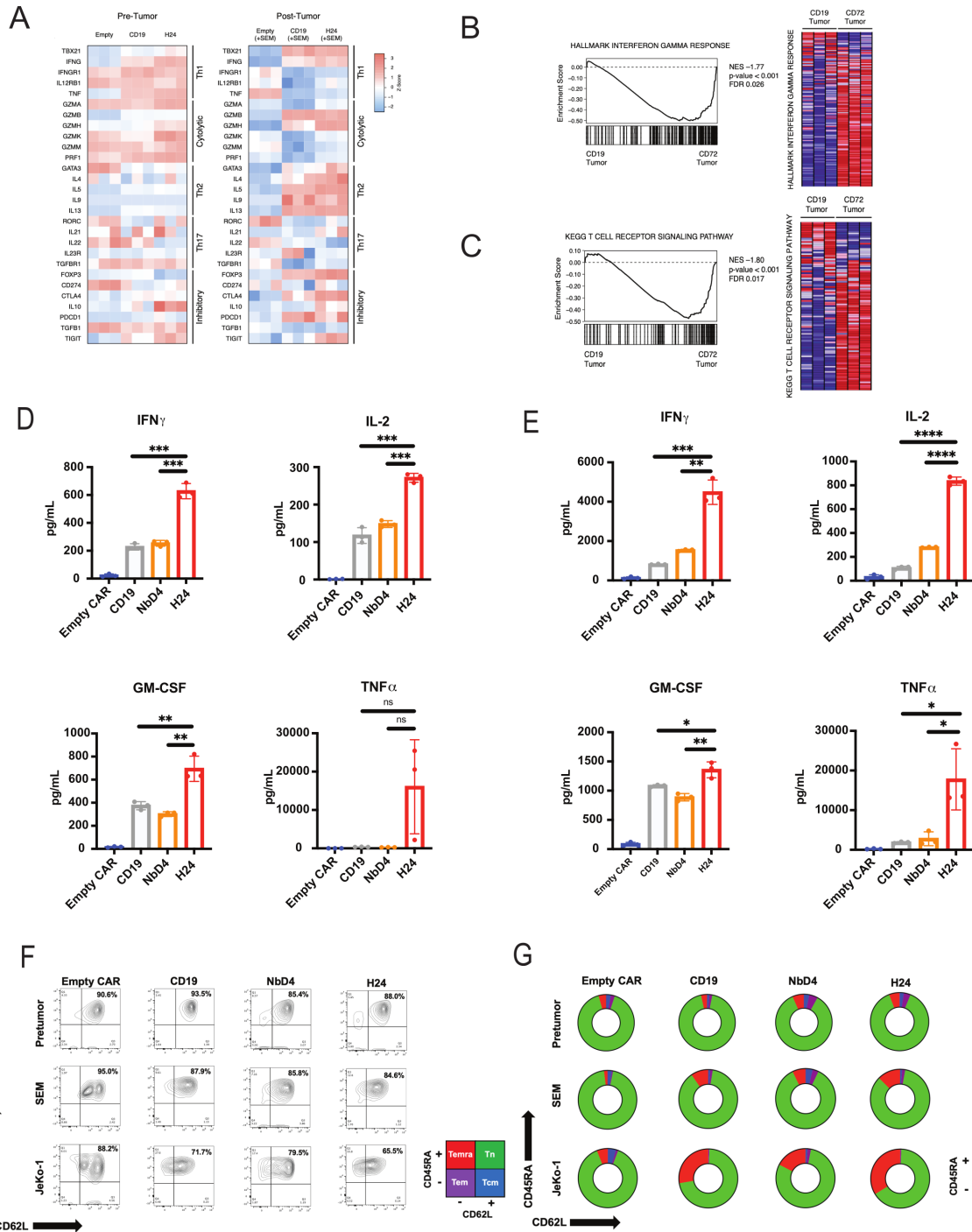


Figure 4 H24 nanoCARs exhibit a unique transcriptional profile compared with CD19 CAR-T cells after exposure to SEM. Bulk RNA-sequencing performed in triplicate on empty CAR, CD19, and H24 CAR-T cells before and after 24-hour exposure to SEM tumor cells. (A) Heat map of genes relevant for T cell differentiation (classified by reference 30) that are differentially expressed between empty CAR, CD19 CAR-T cells, and H24 nanoCARs, either before or after 24 hours SEM exposure (1:1 E:T). (B, C) GSEA plot and heat map of “hallmark interferon gamma response genes” and “KEGG T cell receptor signaling pathway” between CD19 CAR-T cells and H24 nanoCARs after exposure to SEM. (D) Multiplexed cytokine profiling from culture supernatant after 24-hour SEM exposure (n=3 biological replicates). (E) Multiplexed cytokine profiling from culture supernatant after 24-hour Jeko exposure (n=3 biological replicates). (F) Memory marker profiling for CD45RA and CD62L before tumor exposure, after 24-hour exposure to SEM tumor cells, and after 24-hour exposure to JeKo-1 tumor cells. Representative of n=2 technical replicates. (G) Graphical representation of data from figure 4G, in which the number of naïve T cells (CD45RA+/CD62L+), central memory T cells (Tcm: CD45RA-/CD62L+), T-effector memory RA (TEMRA) cells (CD45RA+/CD62L-), and effector memory T cells (Tem: CD45RA-/CD62L-) are shown from the different CAR-T cell constructs in figure 4F. RNA-seq data are publicly deposited to the Gene Expression Omnibus (GEO) repository with accession number: GSE218791.⁵⁰ Data in figure 4D and figure 4E are generated using an unpaired two-tailed t-test. ns=*p<0.05, **p<0.01, ***p<0.001, ****p<0.0001. E:T, effector:tumor; ns, not significant.

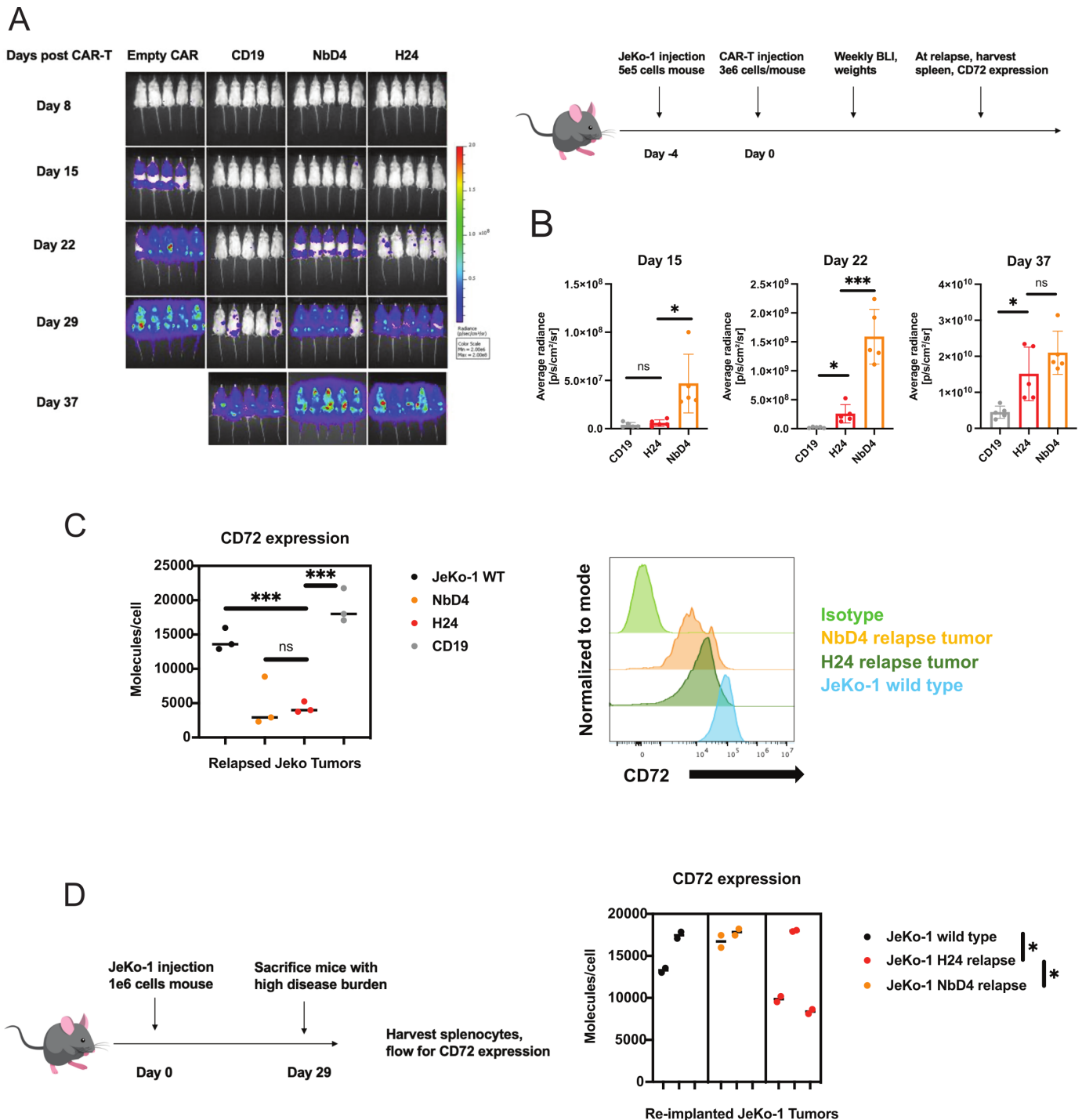


Figure 5 H24 nanoCARs have in vivo lymphoma efficacy and lead to persistent CD72 antigen loss. (A) NSG mice were injected with 5e5 firefly-luciferase labeled JeKo-1 mantle cell lymphoma cells on day -4, and on day 0 mice were treated with 3e6 CAR-T cells per mouse (n=5/arm, as shown). BLI was performed on day -1 to randomize the mice into different treatment arms to ensure the disease burden was equal across all CAR constructs. (B) Tumor burden was assessed weekly via BLI, quantified BLI images on each day after CAR-T cell injection are shown. (C) At sacrifice, quantitative flow cytometry for CD72 expression was performed on relapsed Jeko tumors from n=3 mice/arm. (D) Relapsed JeKo-1 tumors were reimplanted into untreated NSG mice in the absence of anti-CD72 immune pressure. 29 days after reimplantation, quantitative flow cytometry was performed on relapsed Jeko tumors for CD72 expression. Data in figure 5B, figure 5C, and figure 5D are generated using an unpaired two-tailed t-test. ns= $p < 0.05$, *** $p < 0.001$. BLI, biolayer interferometry.

increased signal of recombinant CD72 compared with NbD4 nanoCARs, consistent with increased affinity of the H24 nanobody versus NbD4 (figure 6B, $p < 0.05$).

H24 nanobody is highly specific for CD72 with a reassuring preclinical toxicity profile

Moving toward clinical translation, it is critical to verify

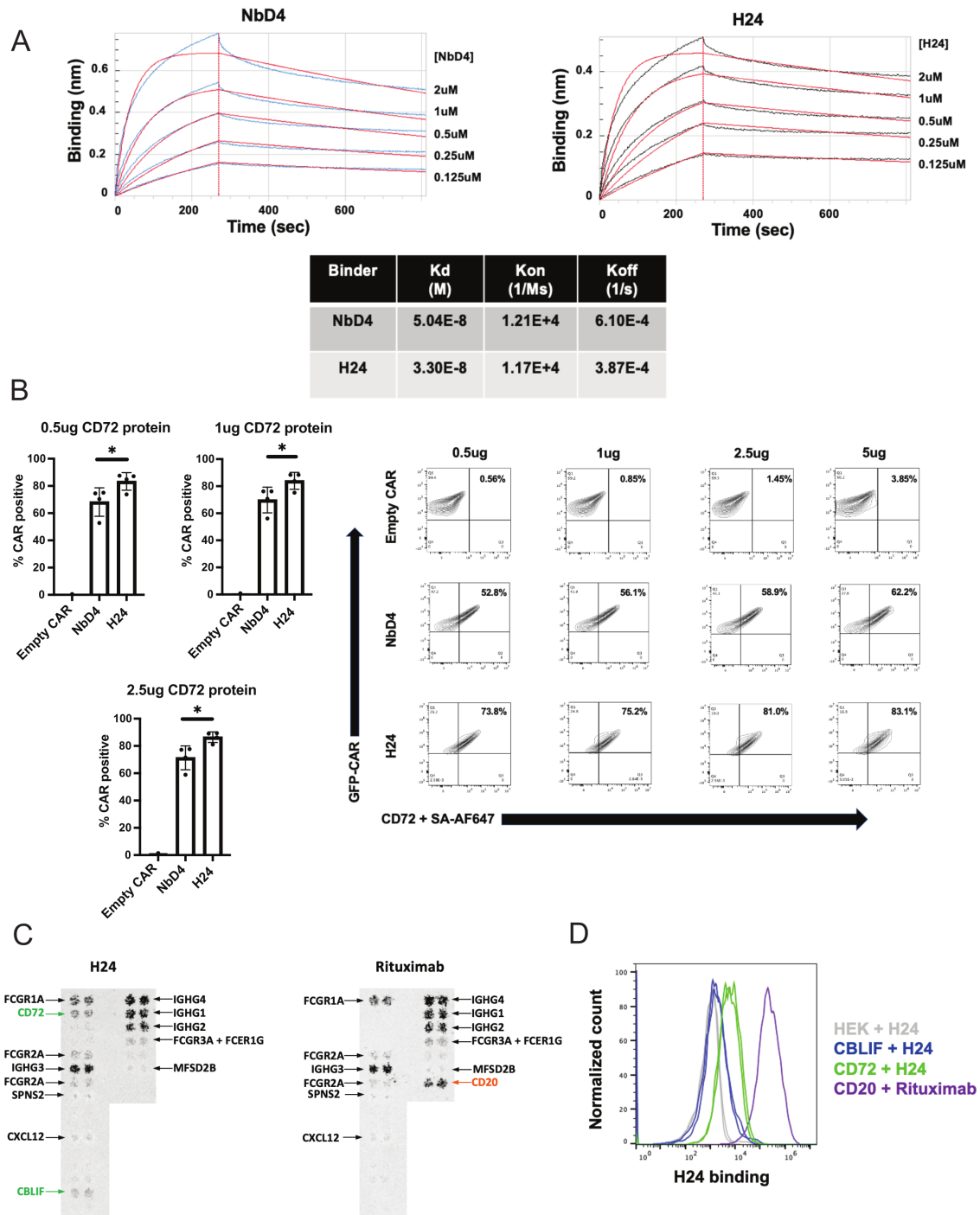


Figure 6 H24 has higher binding affinity to CD72 than NbD4 and is highly specific for CD72. (A) Representative biolayer interferometry plots demonstrating H24 and NbD4 nanobody binding to the biotinylated extracellular domain of CD72. Raw data in black; best fit data from Octet Forte software in red. Data are representative of two technical replicates. Best-fit k_{on} , k_{off} , and calculated K_D are listed. (B) Flow cytometry with recombinant biotinylated CD72 (secondary: streptavidin AF647 conjugate) supports higher affinity of H24 versus NbD4. CAR expression was normalized between all CAR-T cells based on intracellular GFP expression. Bar graphs represent the mean \pm SD for percentage of T cells that are positive for recombinant CD72 binding based on shown gating. Data are representative of two separate experiments from two different T cell donors. (C) HEK cells were engineered to overexpress each of the antigens listed per Retrogenix protocols, and then cells were fixed and evaluated for binding to H24 binder. Possible interactions indicating binding to H24 are shown in green, and non-specific screen hits found with both H24 and rituximab biosimilar in black. (D) HEK cells overexpressing CBLIF, CD72, or wild-type HEK (negative control) were generated per Retrogenix protocols and stained with H24 nanobody-Fc fusion. As a positive control, HEK overexpressing CD20 was stained with rituximab biosimilar. AF647 anti-human IgG Fc detection antibody was used as the secondary antibody for both the H24 and rituximab conditions. H24 binding to CBLIF-expressing cells was considered to be artifactual based on internal validation and assay standards at Retrogenix, given substantial overlap with HEK-alone staining. Data in [figure 6B](#) are generated using an unpaired two-tailed *t*-test. * $p < 0.05$. CBLIF, cobalamin binding intrinsic factor.

that the H24 nanobody sequence does not have any off-target binding to other antigens and solely interacts with CD72. We thus performed nanobody specificity studies using a commercial platform (Retrogenix) evaluating binding to arrayed HEK293 cells overexpressing 6019 individual membrane-spanning proteins. As an important positive control, initial studies on fixed cells confirmed H24 nanobody interaction with CD72. After comparison to rituximab biosimilar to eliminate non-specific screen hits, these findings suggested a potential interaction of H24, but not rituximab, with one other tested protein, cobalamin binding intrinsic factor (CBLIF) (figure 6C). While this protein, located solely within the gastric lumen,⁴¹ is not anticipated to be accessible by circulating CAR-T cells, follow-up confirmatory assays on live cells found the CBLIF hit to be a non-specific artifact of the initial screen, and CD72 was confirmed to be the only validated target of H24 (figure 6D). Supporting this finding of target specificity, incubation of H24 nanoCARs with peripheral blood mononuclear cells from a normal donor found depletion of B-cells, as expected, but no impact on any other profiled normal tissues (online supplemental figure 9A,B) and various immune cell subtypes (online supplemental figure 9C). In vivo toxicity studies revealed no histopathological differences across 14 murine tissues between H24 nanoCARs, CD19 CAR-T, and empty CAR-T (online supplemental table 3). Taken together, these studies support the efficacy and on-target specificity of H24 nanoCARs.

High affinity nanobodies generated by affinity maturation do not improve nanoCAR efficacy

As a moderate increase in binding affinity appeared to increase nanoCAR potency, we investigated whether further increasing anti-CD72 nanobody binding affinity would lead to improved performance. We thus used an affinity maturation strategy via yeast display (online supplemental figure 10A), based on the parental NbD4 CDR sequence (figure 7A), to generate a series of nanobodies with very high affinity for CD72. Notably, in generating our initial library for affinity maturation (see Methods), we not only allowed the CDRs to vary as is typical in these approaches, but also allowed a binary choice at our prior sites of backbone humanization (see figure 7B) between the llama or human sequence. Using flow cytometry-based sorting on yeast, similar to our previously described strategy,⁸ we significantly enriched for nanobodies that bound to 50 pM of input recombinant antigen (online supplemental figure 10B). The selected affinity matured binders had several mutations in the CDRs, as expected, but, remarkably, also converged on several framework mutations also included in H24 (figure 7B). This finding, from a relatively unbiased screen, may suggest the key nanobody framework mutations that drive the higher affinity of H24 versus NbD4.

BLI confirmed the findings from the on-yeast selection, whereby representative, recombinantly expressed clones (NbD4.7, NbD4.13) both demonstrated binding

affinity (K_D) of <1.3 nM (figure 7C), over an order of magnitude higher affinity than either NbD4 or H24. We next incorporated these high affinity binders into the EQ.28z CAR backbone. When evaluated versus either SEM (figure 7D) or JeKo-1 (figure 7E) tumors in vitro, we found no increased cytotoxicity of either NbD4.7 or NbD4.13 nanoCARs when compared with H24, despite much higher affinity for the target CD72. Taken together, these findings support the notion that for single-domain antibodies such as nanobodies, increased binding affinity alone is insufficient to improve CAR-T activity.

DISCUSSION

Our work here underpins the preclinical development and future clinical translation of nanobody-based CAR-T cells (“nanoCARs”) against CD72 for the treatment of patients with relapsed and refractory B-cell malignancies. Surprisingly, we found that humanization of amino acid residues in the framework region alone were able to increase the in vitro and in vivo efficacy of our previously published nanobody design. While these modified residues appeared to drive a moderate increase in affinity for the target CD72, a much greater increase in nanobody affinity did not improve nanoCAR performance. In vitro and in vivo CAR-T characterization, as well as binder specificity screening, supports the clinical translation of “H24”-based CD72 nanoCARs for patients with relapsed and refractory B-cell malignancies.

Toward broader relevance of our findings, nanobody-based CAR-T cells have recently been FDA-approved for multiple myeloma, and several other nanobody-based CAR-T cells have been investigated in the preclinical setting.^{10 16} We note that complete framework humanization is not possible, as it would lead to loss of the obligate monomer properties of the nanobody (see figure 1A). However, as interest in this cell therapy modality accelerates, our work suggests that partial framework humanization, as carried out here, may carry two benefits: (1) reduce potential immunogenicity of llama sequence even further, beyond an already low level compared with murine-origin antibodies, to avoid resistance due to anti-drug antibodies and (2) improving the performance of the CAR-T itself. To the latter point, our work implies that optimization of antibody fragments in CAR-T format should not be limited to modification solely of the CDRs, and, furthermore, obtaining very high affinity nanobodies may be counter-productive. One recent study also made a similar observation after humanizing an anti-CD19 scFv.⁴² This concept necessitates a significant shift in current antibody engineering approaches.

Notably, in both in vitro and in vivo studies, against the SEM B-ALL model, H24 CD72 EQ.28z nanoCARs showed either equivalent or improved performance compared with FMC63 anti-CD19.bbz CAR-T cells (“gold standard” tisagenlecleucel backbone). In vitro against the JeKo-1 lymphoma model, H24 nanoCARs and CD19 CAR-T had equivalent potency, though in vivo CD19 CAR-T cells

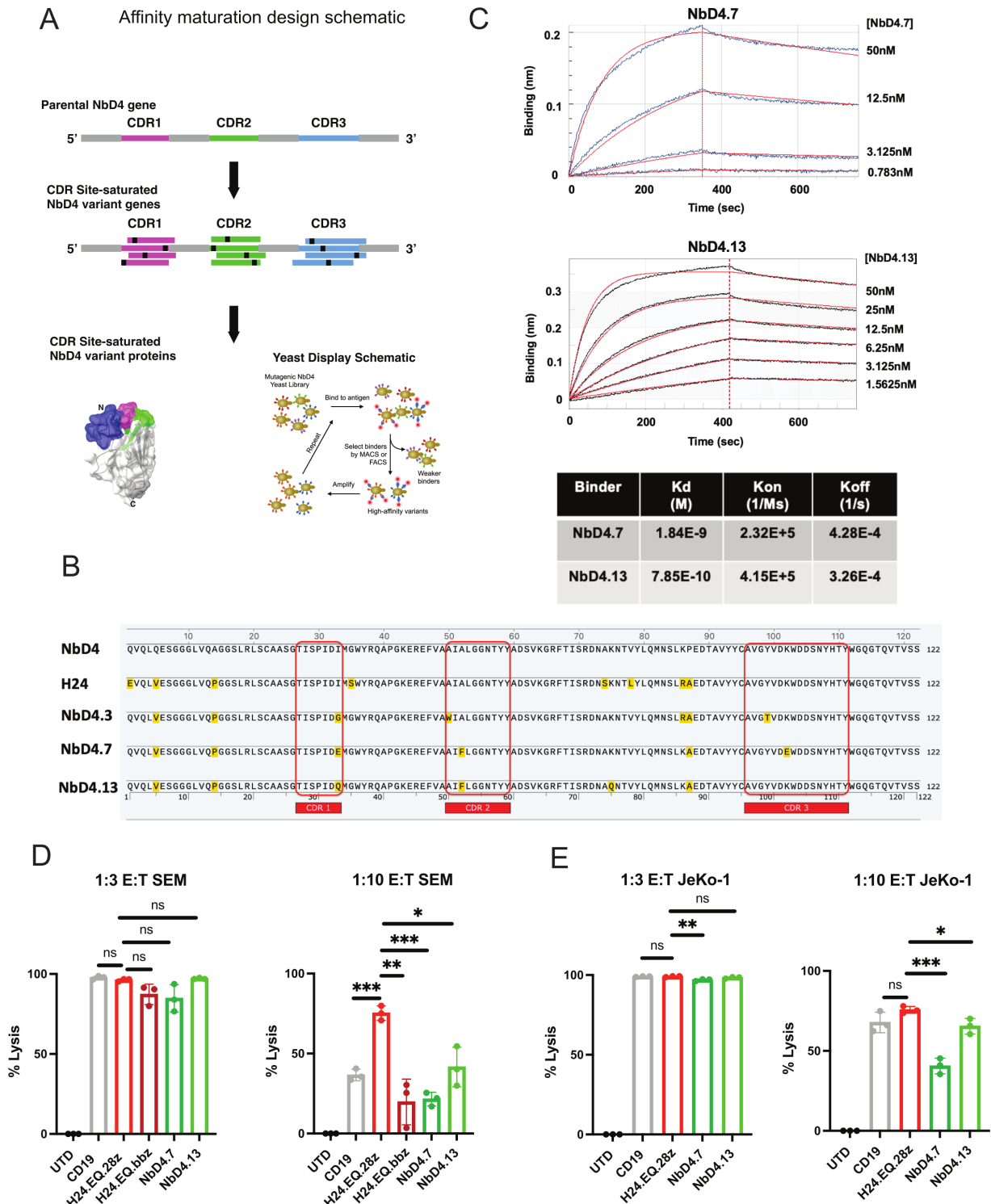


Figure 7 High affinity nanobodies generated by affinity maturation do not improve CAR-T cell efficacy. (A) Schematic for the design of the affinity matured nanobody binders against CD72. (B) Shown are the amino acid sequence alignments of parental NbD4, H24, NbD4.3, NbD4.7, and NbD4.13. Amino acids in red are mutations that are in either the CDRs or the framework regions that are different than parental NbD4. (C) Representative bi-layer interferometry plots demonstrating NbD4.7 and NbD4.13 binding to the biotinylated extracellular domain of CD72. Raw data is in blue for NbD4.7 and black for NbD4.13, while best fit data is in red. Data are representative of two independent experiments. (D) In vitro 24 hours cytotoxicity assay against SEM comparing affinity matured nanoCARs NbD4.7 and NbD4.13 to H24.EQ.28z at E:T 1:3 and 1:10, cocultured for 24 hours. Data normalized to untransduced T cells (UTD) co-cultured with SEM at the indicated E:T ratios. n=3 technical replicates per data point. (E) In vitro 24 hours cytotoxicity assay against JeKo-1 comparing affinity matured nanoCARs NbD4.7 and NbD4.13, both with EQ.28z backbone, to H24.EQ.28z at various E:T ratios (1:3, 1:10). Data normalized to untransduced T cells (UTD) cocultured with JeKo-1 at the indicated E:T ratios. n=3 technical replicates per data point. Data in [figure 7D](#) and [figure 7E](#) are generated using an unpaired two-tailed t-test. ns= $p < 0.05$, ** $p < 0.01$, *** $p < 0.001$. E:T, effector:tumor.



could still outperform H24 nanoCARs. These results, together with additional characterization described above, support the clinical translation of H24 CD72 nanoCARs for patients relapsing after CD19 CAR-T. We have initiated necessary studies at our institution to pursue an Investigational New Drug application and a subsequent Phase I clinical trial.

New treatment options are urgently needed for these patients relapsing after CD19-directed therapy, particularly as CD22-directed CAR-T alone, without HSCT, have not been curative in this population.⁷ Current CD22 scFv-based CARs may suffer from diminished performance due to the specific linkage between the heterodimeric V_H and V_L domains.¹¹ As nanobodies are obligate monomers, we anticipate that similar complications will not exist for CD72 nanoCARs. That said, however, antigen downregulation, also frequently seen with CD22-targeting CAR-T,⁷ may remain a significant clinical hurdle, and will need to be investigated in clinical trials. Recent studies from an independent group confirmed that essentially all pediatric B-cell tumors express CD72, including after relapse on CD19-directed therapies, and, remarkably, a majority of pediatric acute myeloid leukemia specimens were also positive for this antigen.⁴³ Future work will aim to incorporate new engineering strategies^{44–46} to design cell therapies to target tumors with even lower antigen density, as well as investigate mechanisms of CD72 downregulation and potential cotargeting strategies to overcome this phenomenon.⁸

In general, while extensive work has gone into optimizing the signaling-relevant domains of CAR-T cells, much less has been investigated regarding optimal properties of CAR-T antibody binders. Our results endorse a “goldilocks” model of nanobody optimization, previously only demonstrated for scFv-based CAR-T,¹⁴ whereby nanobodies with moderate affinity for CD72 ($K_D \sim 10\text{--}50\text{ nM}$) outperform those with sub-nM affinity. The biological mechanisms underlying the diminished performance of high affinity binders remain to be unraveled, though they may relate to CAR-T cell processivity of killing or increased trogocytosis at high target affinity.^{47,48}

In terms of limitations, our results here have only been applied to anti-CD72 nanobodies generated in our group. Future work will investigate whether the same framework mutations identified here uniformly improve nanobody-based CAR-T performance, or whether beneficial framework modifications are specific to each binder sequence and/or target. Furthermore, while our prior target expression analyses,⁸ binder specificity studies, and in vitro cytotoxicity assays versus normal tissues (online supplemental figure 8,9)) support a strong safety profile of targeting CD72, clinical studies are required to demonstrate both the safety and efficacy of our H24 nanoCARs. As we found that CD72 expression appeared higher than CD22 on two adult B-ALL patient tumors who relapsed after tisagenlecleucel (figure 3G,H), a more thorough comparison of CD72 and CD22 as B-ALL targets will be an interesting topic for a future study. Our RNA-seq and

flow cytometric data suggest that CD72 nanoCARs may express slightly higher exhaustion markers and have less naïve T cells than CD19.bbz CAR-T cells. This phenotype will need to be more thoroughly evaluated in the eventual CD72 nanoCAR clinical trial. Furthermore, we found that H24 nanoCARs do not always outperform CD19 CAR-T cells in vivo; however, this comparison may not be relevant in terms of future clinical translation, as H24 nanoCARs will be administered in patients who relapse after CD19 CAR-T cell treatment.

In conclusion, our results support a paradigm shift in antibody design for cell therapies, whereby alterations of the framework, not just CDRs, must also be considered when optimizing antibody recognition domains. This strategy, designed to reduce immunogenicity, serendipitously led to an improved anti-CD72 cell therapy with a reassuring preclinical toxicity profile that may be a viable therapeutic option for patients who relapse after CD19-directed immunotherapy.

Author affiliations

¹Department of Pediatrics, Division of Hematology/Oncology, University of California, UCSF Benioff Children's Hospital, San Francisco, California, USA

²Department of Pediatrics, Division of Allergy, Immunology, and Bone Marrow Transplantation, University of California, UCSF Benioff Children's Hospital, San Francisco, California, USA

³Department of Laboratory Medicine, University of California, San Francisco, California, USA

⁴Helen Diller Family Comprehensive Cancer Center, University of California, San Francisco, California, USA

⁵Department of Medicine, Division of Hematology and Blood and Marrow Transplantation, University of California, San Francisco, California, USA

⁶Department of Bioengineering and Therapeutic Sciences, University of California, San Francisco, California, USA

⁷Chan Zuckerberg Biohub, San Francisco, California, USA

Twitter Gianina Wicaksono @giawicak

Contributors WCT: conceptualization, data curation, formal analysis, funding acquisition, validation, investigation, visualization, methodology, writing-original draft, writing-review and editing. MAN: conceptualization, data curation, formal analysis, validation, investigation, visualization, methodology, writing-review and editing. AN: Data curation, formal analysis, validation, investigation, writing-review and editing. AI: Data curation, validation, investigation, writing-review and editing. BJH: data curation, formal analysis, validation, visualization, methodology, writing-review and editing. GW: data curation, validation, investigation, writing-review and editing. PP: data curation, validation, writing-review and editing. JACS: Data curation, validation, writing-review and editing. EPY: data curation, formal analysis, validation, methodology, writing-review and editing. ER: data curation, validation, methodology, writing-review and editing. FS: data curation, validation, writing-review and editing. VS: data curation, validation, writing-review and editing. MH: supervision, writing-review and editing. ACL: resources, writing-review and editing. ES: Resources, supervision, funding acquisition, writing-review and editing. APW: conceptualization, resources, methodology, supervision, funding acquisition, writing-original draft, writing-review and editing, guarantor.

Funding This work was supported by the Dept. of Defense Congressionally Directed Medical Research Program W81XWH2210807, California Institute of Regenerative Medicine TRAN1-12987, and UCSF Living Therapeutics Initiative (to APW); the National Institute of Health T32 Research Training in Childhood Cancer (T32CA128583), the Chan Zuckerberg Biohub Physician-Scientist Fellowship Program, and the American Society of Hematology Research Training Award for Fellows (to WCT); NIH/NCI P30 CA082103 (to UCSF Helen Diller Family Comprehensive Cancer Center Preclinical Therapeutic Core Facility, managed by VS; support of the Laboratory for Cell Analysis; support for Pediatric Malignancies Tissue Bank, directed by ES); Alex's Lemonade Stand Foundation Center of Excellence (to ES); BP28 Foundation (to MH). We thank the staff of Retrogenix/

Charles River Laboratories UK for performing noted analyses and providing figures and methods for publication.

Competing interests APW and MAN have filed intellectual property claims relevant to the nanobody sequences described here. MAN is an employee and equity shareholder of Cartography Biosciences. APW has received research funding from Genentech/Roche. The other authors declare no relevant conflicts of interest.

Patient consent for publication Not applicable.

Provenance and peer review Not commissioned; externally peer reviewed.

Data availability statement Data are available in a public, open access repository. All data relevant to the study are included in the article or uploaded as online supplemental information. All data relevant to the study are included in the article or uploaded as online supplemental information. RNA-seq data are publicly deposited to the Gene Expression Omnibus (GEO) repository with accession number: GSE218791, and the persistent URL is: <https://www.ncbi.nlm.nih.gov/geo/query/acc.cgi?acc=GSE218791>. There are no conditions of reuse.

Supplemental material This content has been supplied by the author(s). It has not been vetted by BMJ Publishing Group Limited (BMJ) and may not have been peer-reviewed. Any opinions or recommendations discussed are solely those of the author(s) and are not endorsed by BMJ. BMJ disclaims all liability and responsibility arising from any reliance placed on the content. Where the content includes any translated material, BMJ does not warrant the accuracy and reliability of the translations (including but not limited to local regulations, clinical guidelines, terminology, drug names and drug dosages), and is not responsible for any error and/or omissions arising from translation and adaptation or otherwise.

Open access This is an open access article distributed in accordance with the Creative Commons Attribution Non Commercial (CC BY-NC 4.0) license, which permits others to distribute, remix, adapt, build upon this work non-commercially, and license their derivative works on different terms, provided the original work is properly cited, appropriate credit is given, any changes made indicated, and the use is non-commercial. See <http://creativecommons.org/licenses/by-nc/4.0/>.

ORCID iD

William C Temple <http://orcid.org/0000-0003-3375-2703>

REFERENCES

- Maude SL, Frey N, Shaw PA, *et al.* Chimeric antigen receptor T cells for sustained remissions in leukemia. *N Engl J Med* 2014;371:1507–17.
- Maude SL, Laetsch TW, Buechner J, *et al.* Tisagenlecleucel in children and young adults with B-cell Lymphoblastic leukemia. *N Engl J Med* 2018;378:439–48.
- Majzner RG, Mackall CL. Clinical lessons learned from the first leg of the CAR T cell journey. *Nat Med* 2019;25:1341–55.
- Schultz LM, Eaton A, Baggott C, *et al.* Outcomes after Nonresponse and relapse post-Tisagenlecleucel in children, adolescents, and young adults with B-cell acute Lymphoblastic leukemia. *JCO* 2023;41:354–63.
- Wudhikarn K, Flynn JR, Rivière I, *et al.* Interventions and outcomes of adult patients with B-ALL progressing after Cd19 Chimeric antigen receptor T-cell therapy. *Blood* 2021;138:531–43.
- Chow VA, Gopal AK, Maloney DG, *et al.* Outcomes of patients with large B-cell Lymphomas and progressive disease following Cd19-specific CAR T-cell therapy. *Am J Hematol* 2019;94:E209–13.
- Shah NN, Highfill SL, Shalabi H, *et al.* Cd4/Cd8 T-cell selection affects Chimeric antigen receptor (CAR) T-cell potency and toxicity: updated results from a phase I anti-Cd22 CAR T-cell trial. *JCO* 2020;38:1938–50.
- Nix MA, Mandal K, Geng H, *et al.* Surface Proteomics reveals Cd72 as a target for in vitro-evolved Nanobody-based CAR-T cells in Kmt2A/Mll1-rearranged B-ALL. *Cancer Discov* 2021;11:2032–49.
- Tsubata T. Inhibitory B cell Co-receptors and autoimmune diseases. *Immunol Med* 2019;42:108–16.
- Bao C, Gao Q, Li L-L, *et al.* The application of Nanobody in CAR-T therapy. *Biomolecules* 2021;11:238.
- Singh N, Frey NV, Engels B, *et al.* Antigen-independent activation enhances the efficacy of 4-1Bb-Costimulated Cd22 CAR T cells. *Nat Med* 2021;27:842–50.
- Schmid DA, Irving MB, Posevitz V, *et al.* Evidence for a TCR affinity threshold delimiting maximal Cd8 T cell function. *The Journal of Immunology* 2010;184:4936–46.
- Thomas S, Xue SA, Bangham CRM, *et al.* Human T cells expressing affinity-matured TCR display accelerated responses but fail to recognize low density of MHC-peptide antigen. *Blood* 2011;118:319–29.
- Ghorashian S, Kramer AM, Onuoha S, *et al.* Enhanced CAR T cell expansion and prolonged persistence in pediatric patients with ALL treated with a low-affinity Cd19 CAR. *Nat Med* 2019;25:1408–14.
- Berdeja JG, Madduri D, Usmani SZ, *et al.* Ciltacabtagene Autoleucl, a B-cell maturation antigen-directed Chimeric antigen receptor T-cell therapy in patients with Relapsed or refractory multiple myeloma (CARTITUDE-1): a phase 1B/2 open-label study. *The Lancet* 2021;398:314–24.
- Safarzadeh Kozani P, Naseri A, Mirarefin SMJ, *et al.* Nanobody-based CAR-T cells for cancer Immunotherapy. *Biomark Res* 2022;10:24.
- Martin T, Usmani SZ, Schecter JM, *et al.* Matching-adjusted indirect comparison of efficacy outcomes for Ciltacabtagene Autoleucl in CARTITUDE-1 versus Idecabtagene Vicleucl in Karma for the treatment of patients with Relapsed or refractory multiple myeloma. *Curr Med Res Opin* 2021;37:1779–88.
- Zhu L, Yang X, Zhong D, *et al.* Single-domain antibody-based TCR-like CAR-T: A potential cancer therapy. *Journal of Immunology Research* 2020;2020:1–8.
- An N, Hou YN, Zhang QX, *et al.* Anti-multiple myeloma activity of Nanobody-based anti-Cd38 Chimeric antigen receptor T cells. *Mol Pharm* 2018;15:4577–88.
- Han L, Zhang J-S, Zhou J, *et al.* Single VHH-directed BCMA CAR-T cells cause remission of Relapsed/refractory multiple myeloma. *Leukemia* 2021;35:3002–6.
- Wagner DL, Fritsche E, Pulsipher MA, *et al.* Immunogenicity of CAR T cells in cancer therapy. *Nat Rev Clin Oncol* 2021;18:379–93.
- Maus MV, Haas AR, Beatty GL, *et al.* T cells expressing Chimeric antigen receptors can cause Anaphylaxis in humans. *Cancer Immunol Res* 2013;1:26–31.
- Turtle CJ, Hanafi L-A, Berger C, *et al.* Cd19 CAR-T cells of defined Cd4+ Cd8+ composition in adult B cell ALL patients. *J Clin Invest* 2016;126:85309:2123–38..
- Greenman R, Pizem Y, Haus-Cohen M, *et al.* Shaping functional avidity of CAR T cells: affinity, avidity, and antigen density that regulate response. *Mol Cancer Ther* 2021;20:872–84.
- Duan Y, Chen R, Huang Y, *et al.* Tuning the ignition of CAR: optimizing the affinity of scFv to improve CAR-T therapy. *Cell Mol Life Sci* 2022;79.
- Jonnalagadda M, Mardiros A, Urak R, *et al.* Chimeric antigen receptors with Mutated IgG4 FC spacer avoid FC receptor binding and improve T cell persistence and antitumor efficacy. *Molecular Therapy* 2015;23:757–68.
- Wang D, Starr R, Chang W-C, *et al.* Chlorotoxin-directed CAR T cells for specific and effective targeting of glioblastoma. *Sci Transl Med* 2020;12:eaaw2672.
- Vincke C, Loris R, Saerens D, *et al.* General strategy to humanize a Camelid single-domain antibody and identification of a universal Humanized Nanobody scaffold. *J Biol Chem* 2009;284:3273–84.
- Cappell KM, Kochenderfer JN. A comparison of Chimeric antigen receptors containing Cd28 versus 4-1Bb Costimulatory domains. *Nat Rev Clin Oncol* 2021;18:715–27.
- Wu Y, Biswas D, Usaite I, *et al.* A local human Vδ1 T cell population is associated with survival in Nonsmall-cell lung cancer. *Nat Cancer* 2022;3:696–709.
- Chen GM, Chen C, Das RK, *et al.* Integrative bulk and single-cell profiling of Premanufacture T-cell populations reveals factors mediating long-term persistence of CAR T-cell therapy. *Cancer Discov* 2021;11:2186–99.
- Selli ME, Landmann JH, Terekhova M, *et al.* Costimulatory domains direct distinct fates of CAR-driven T-cell dysfunction. *Blood* 2023;141:3153–65.
- Sotillo E, Barrett DM, Black KL, *et al.* Convergence of acquired mutations and alternative splicing of Cd19 enables resistance to CART-19 Immunotherapy. *Cancer Discov* 2015;5:1282–95.
- Sommermeier D, Hill T, Shamah SM, *et al.* Fully human Cd19-specific Chimeric antigen receptors for T-cell therapy. *Leukemia* 2017;31:2191–9.
- Grupp SA, Kalos M, Barrett D, *et al.* Chimeric antigen receptor-modified T cells for acute Lymphoid leukemia. *N Engl J Med* 2013;368:1509–18.
- Lamble AJ, Myers RM, Taraseviciute A, *et al.* Preinfusion factors Impacting relapse Immunophenotype following Cd19 CAR T cells. *Blood Adv* 2023;7:575–85.
- Xu X, Sun Q, Liang X, *et al.* Mechanisms of relapse after Cd19 CAR T-cell therapy for acute Lymphoblastic leukemia and its prevention and treatment strategies. *Front Immunol* 2019;10:2664.



- 38 Cheng J, Zhao L, Zhang Y, *et al.* Understanding the mechanisms of resistance to CAR T-cell therapy in malignancies. *Front Oncol* 2019;9:1237.
- 39 Schmidts A, Maus MV. Making CAR T cells a solid option for solid tumors. *Front Immunol* 2018;9:2593.
- 40 Shah NN, Fry TJ. Mechanisms of resistance to CAR T cell therapy. *Nat Rev Clin Oncol* 2019;16:372–85.
- 41 Howard TA, Misra DN, Grove M, *et al.* Human gastric intrinsic factor expression is not restricted to Parietal cells. *J Anat* 1996;189:303–13.
- 42 Dwivedi A, Karulkar A, Ghosh S, *et al.* Robust antitumor activity and low cytokine production by novel Humanized anti-Cd19 CAR T cells. *Mol Cancer Ther* 2021;20:846–58.
- 43 Buldini B, Faggin G, Porcù E, *et al.* Cd72 is a pan-tumor antigen associated with childhood acute leukemia. *Blood* 2022;140:4974–5.
- 44 Mansilla-Soto J, Eyquem J, Haubner S, *et al.* HLA-independent T cell receptors for targeting tumors with low antigen density. *Nat Med* 2022;28:345–52.
- 45 Hou AJ, Chen LC, Chen YY. Navigating CAR-T cells through the solid-tumour Microenvironment. *Nat Rev Drug Discov* 2021;20:531–50.
- 46 Feucht J, Sun J, Eyquem J, *et al.* Publisher correction: calibration of CAR activation potential directs alternative T cell fates and therapeutic potency. *Nat Med* 2019;25:530.
- 47 Hamieh M, Dobrin A, Cabriolu A, *et al.* CAR T cell Trophocytosis and cooperative killing regulate tumour antigen escape. *Nature* 2019;568:112–6.
- 48 Olson ML, Mause ERV, Radhakrishnan SV, *et al.* Low-affinity CAR T cells exhibit reduced Trophocytosis, preventing rapid antigen loss, and increasing CAR T cell expansion. *Leukemia* 2022;36:1943–6.
- 49 Källberg M, Wang H, Wang S, *et al.* Template-based protein structure modeling using the RaptorX web server. *Nat Protoc* 2012;7:1511–22.
- 50 Temple WC, Huang BJ, Wiita AP. Framework Humanization increases the affinity and potency of anti-Cd72 Nanobody-based CAR-T cells for B-cell malignancies. Available: <https://www.ncbi.nlm.nih.gov/geo/query/acc.cgi?acc=GSE218791> [Accessed 29 Dec 2022].